

AN AUTOML-BASED COMPARATIVE EVALUATION OF MACHINE LEARNING METHODS FOR DETECTION OF ECCENTRICITY FAULTS IN INDUCTION MOTORS BY USING VIBRATION SIGNALS

Eyüp Irgat¹⁾, Abdurrahman Ünsal²⁾

1) Department of Kutahya Technical Sciences Vocational School, Kutahya Dumlupinar University, Evliya Celebi Campus, 43100 Kutahya, Turkey (✉ eyup.irgat@dpu.edu.tr)

2) Department of Electrical Electronics Engineering, Kutahya Dumlupinar University, Evliya Celebi Campus, 43100 Kutahya, Turkey

Abstract

Induction motors (IMs) are the most widely used electrical machines in industrial applications. However, they are subject to various mechanical and electrical faults. Eccentricity faults are among the common mechanical faults of IMs. This study compares the performance of four commonly used *machine learning* (ML) methods, including *k-nearest neighbours* (k-NN), *decision tree* (DT), *support vector machine* (SVM), and *random forest* (RF) along with the statistical features in detecting eccentricity faults of IMs with an *automated machine learning* (AutoML) model. The aim of using AutoML in this study is to fully automate the process of detection of eccentricity faults of IMs by selecting the classifier with the highest accuracy rate and shortest computation time along with the most effective feature(s). The eccentricity fault analysed in this study was experimentally implemented in the laboratory. Three-axis vibration signals were collected for healthy and eccentricity-faulty IMs. In the proposed study the three-axis vibration signals are pre-processed to determine the statistical features that are used as input to the ML methods. The proposed study offers the best ML method among the four studied algorithms and the need for expert knowledge of ML and eccentricity fault detection. The proposed AutoML model offers the DT method along with the z-axis rms feature for the highest accuracy rate and the shortest computation time in detecting the eccentricity fault.

Keywords: Induction motors, eccentricity faults, machine learning techniques, fault detection, vibration analysis, AutoML.

1. Introduction

Electrical motors are the most widely used electrical machines in industrial applications. *Induction motors* (IMs) are the most popular electrical motors. IMs are preferred due to their low cost, high reliability, and simplicity. However, despite their advantages, IMs are not free from faults. Unexpected faults of IMs can lead to interruptions in production lines, significant

financial losses, and reduced revenues. The accurate detection and diagnosis of faults of IMs prevent undesired results and long downtimes [1]. The faults in IMs can be broadly classified into mechanical and electrical ones. The mechanical faults in IMs include air gap eccentricity, misalignment, bearing faults, and gearbox-related faults. The electrical faults are related to the stator and rotor. Stator-related faults consist of open-circuit, short-circuit, and insulation failure, while rotor-related ones consist of broken rotor bars and broken or cracked end-rings. There are various surveys on the distribution and root cause of faults of IMs [2–4]. These surveys show that the distribution and root cause of faults vary with the power rating and the supply voltage of IMs. The distribution of the faults in 0.75 kW to 150 kW IMs is given in Fig. 1 [4].

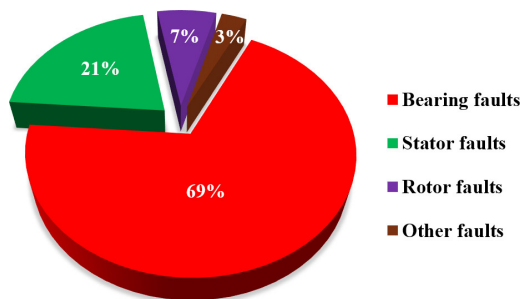


Fig. 1. Distribution of faults in IMs.

Eccentricity faults occur due to an imbalanced distance in the air gap between the rotor and stator. Due to the short air-gap distance of IMs, the changes originating from eccentricity in the air gap are more important than in other machines. Even though the percentage of eccentricity faults is comparatively lower than the percentage of other faults of IMs, they may lead to other types of faults, such as bearing faults and bending of the motor shaft, which in turn, may lead to excessive vibration and increased temperature. In addition, the rotor may rub the stator and damage the lamination and windings [5–7]. Therefore, this study focuses on the detection of eccentricity faults.

The fault diagnosis methods in IMs can be classified as model-based, signature-extraction-based, and knowledge-based. The model-based methods are based on the mathematical models of IMs. The signature-extraction-based methods extract the relevant signatures from monitoring signals. The knowledge-based methods are based on ML models used in this study.

The most widely utilized monitoring signals for detecting faults of IMs include stator current, voltage, vibration, air-gap torque, angular speed, instantaneous power, and magnetic flux signals. The monitoring signals can be processed in the time-domain, frequency-domain [8, 9], or time-frequency [10–13] domains to detect the faults of IMs. Statistical features such as rms, crest factor, kurtosis, spectral kurtosis, skewness, peak value, p2p value, shape factor, impulse factor, and clearance factor are employed in the time-domain analysis to assess the health of IMs [14]. The frequency-domain methods provide successful results in the analysis of stationary signals. Nevertheless, they are ineffective in analysing nonstationary signals where the spectrum and period of the signals change. In the analysis of nonstationary signals, time-frequency analysis methods are preferred.

The *Fast Fourier transform* (FFT) based methods are among the commonly used frequency-domain-based signal processing methods [15]. *Continuous wavelet transform* (CWT) [16], *empirical mode decomposition* (EMD) [17, 18], *discrete wavelet transform* (DWT) [19, 20], and *wavelet packet transform* (WPT) [21] and their variants are commonly used time-frequency domain methods. Time-domain methods use statistical features along with ML models in the detection of faults.

An experimental comparison of various ML-based classification methods for detecting rotor faults of IMs is presented in [22]. The study uses time-domain and frequency-domain features of current signals. The performance of the study is evaluated by processing the stator current signals of an IM under various loading levels based on ML classification methods. A comprehensive review of condition monitoring of IMs based on ML methods is presented in [23].

The widely used ML methods are k-NN, DT [24], SVM [25], RF methods [26], *principal component analysis* (PCA) [27], *artificial neural networks* (ANN) [28–30], and *singular value decomposition* (SVD) [31].

The use of ML for a specific detecting or classification task requires expert knowledge in the field of both the task and ML to choose the appropriate classifier and the best feature(s) with respect to accuracy rate and computation time. Manually selecting the appropriate classifier and the best feature(s) for the detection of faults of IMs with various signals requires expert knowledge and a longer computation time.

The proposed study compares the performance of four ML methods, including k-NN, DT, SVM, and RF, using the AutoML model to detect the eccentricity faults of IMs using three-axis vibration signals concerning the accuracy rate and computation time along with the statistical features.

The contribution of the proposed study is to determine the most effective feature(s) and the ML method with the highest accuracy rate and shortest computation time automatically and reduce the need for expert knowledge in fault detection.

The paper is organized as follows: Section 2 briefly reviews the classification methods and data pre-processing. Sections 3 and 4 describe the implementation of the eccentricity faults and data collection system, respectively. The details of the proposed AutoML model are given in Section 5. The results and the performance of the proposed method are described in Section 6. The paper concludes with Section 7.

2. Classification methods and data pre-processing

Machine learning methods have been widely used in detecting and classifying faults of IMs in recent years [32]. ML methods are mainly preferred in analysing vibration signals (which are nonstationary) for the detection of faults of IMs.

2.1. Classification methods

Four different ML-based classification methods, including k-NN, DT, SVM, and RF, are used in this study. Each of these methods is described below.

2.1.1. K-nearest neighbours

The k-NN algorithm is a supervised ML algorithm. Recently, it has been widely used to solve classification problems. The k-NN algorithm is a nonparametric classifier. It does not need a training model for implementation and is therefore referred to as a lazy learner. Each dataset is labelled based on its n-classifications. The method evaluates the similarity among new and present datasets. The k parameter, generally an odd number, is the number of nearest neighbours [33]. A sample classification process of the k-NN algorithm structure is given in Fig. 2. The k parameter of the k-NN algorithm is tuned by an iterative search method. The search method is performed on a randomly selected twofold separate dataset called train and test in each iteration. The k-NN classification tasks are performed for both the test and training dataset separately by varying the value of k from 2 to 10, as shown in Fig. 3. The value of k is chosen as 3 based on the results given

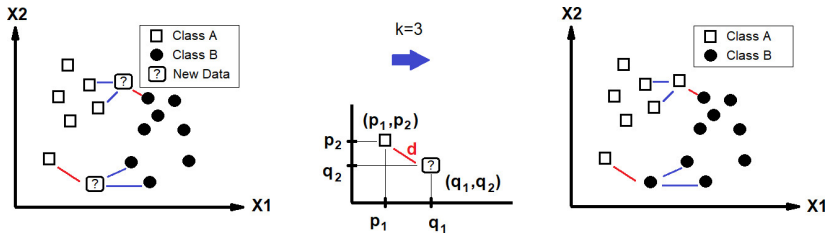


Fig. 2. A sample classification process of the k-NN algorithm.

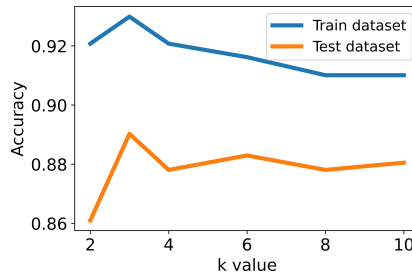


Fig. 3. Determination of the k parameter in the k-NN classifier model in the proposed study.

in Fig. 3. The new data class is determined by calculating the distance to its 3-nearest neighbours. Euclidean, Manhattan, and Minkowski are the distance methods used in k-NN. The Euclidean distance method is used in this study. It can be calculated in (1) and (2).

$$d(p, q) = \sqrt{\sum_{i=1}^n (p_i - q_i)^2}, \quad (1)$$

$$d = \sqrt{(q_1 - p_1)^2 + (p_2 - q_2)^2}, \quad (2)$$

where p_i is the existing data point, q_i is the new data point, n is the number of dimensions, and d is the Euclidean distance.

2.1.2. Decision tree

The decision tree, a widely used classification algorithm in data mining and ML [24], reaches a decision and conclusion with a tree model. The tree model has nodes and branches. Branches are formed by the decisions made at the node. The last nodes of the tree are called leaf nodes. A classification label is assigned to the leaf nodes. Optimum points separate the classes. Figure 4 shows the separation process of the classes in the DT algorithm. The location of the data based on the optimum points is evaluated with the DT. The classification is evaluated at the extreme point of the DT. DT naturally supports classification problems with more than two classes. The most commonly used measures for DT are the Entropy and Gini indexes given in (3) and (4) [34].

$$E = - \sum_{i=1}^n x_i \log_2(x_i), \quad (3)$$

$$Gini = 1 - \sum_{i=1}^n x_i^2, \quad (4)$$

where x_i is the probability corresponding to n possible states.

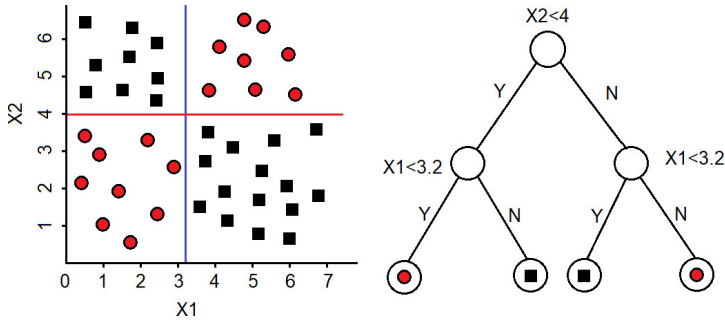


Fig. 4. Sample of the separation process of the classes in the DT algorithm.

2.1.3. Support vector machine

Support vector machine is a statistical learning theory-based, effective, and flexible supervised ML algorithm widely used in classifying, regression, and detecting outliers [35]. As can be seen in Fig. 5, SVM generates hyperplanes that correctly separate the classes. Support vectors can be defined as the data points closest to the hyperplane. The location of the dividing line is determined based on data points. The *optimal hyperplane* (OH) is the decision plane that divides the different classes. Max. Margin is the maximum distance between support vectors of other classes (Fig. 5). The classes above the *positive hyperplane* (PH) belong to healthy and those below the *negative hyperplane* (NH) belong to faulty (healthy class refers to healthy IM, faulty class refers to eccentricity-faulty IM). The OH, PH, NH, and maximum margin can be calculated by (5). This study uses a *support vector classifier* (SVC) based on the SVM library.

$$\begin{aligned}
 \text{OH; } & \vec{w} \cdot \vec{x} + b = 0, \\
 \text{PH; } & \vec{w} \cdot \vec{x} + b = 1, \\
 \text{NH; } & \vec{w} \cdot \vec{x} + b = -1, \\
 \text{max, marg} & = 2/\|w\|,
 \end{aligned}
 \tag{5}$$

where \vec{w} is the weight, \vec{x} is the data value, and b is the bias.

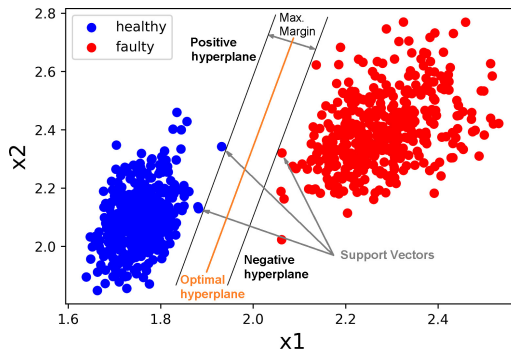


Fig. 5. A sample of the decision plane that divides the different classes in the SVM algorithm.

2.1.4. Random forest

Random forest is a tree-based ensemble learning method [36] that uses multiple decision tree structures to make decisions. Each node in the DT operates on a random subset of features to calculate the output. The structure of the RF classifier used in the proposed study is given in Fig. 6, and details of the RF can be found in [26].

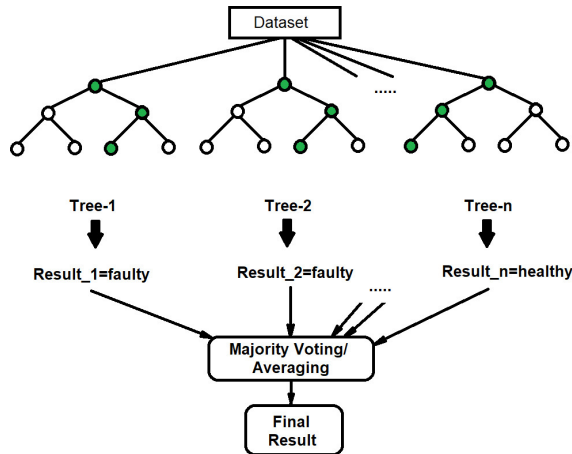


Fig. 6. RF algorithm structure.

The parameters of classifiers, including k-NN, DT, SVC, and RF, used in the proposed study are given in Table 1. The values of the parameters were chosen by trial and error with respect to the optimum performance of classifiers.

Table 1. Parameters of classifiers.

Classifier	Parameter	Value
k-NN	k	3
	weights	uniform
	algorithm	auto
	metric	Euclidean
DT	max_depth	5
SVC	kernel	linear
RF	n_estimators	10
	max_depth	5

2.2. Data pre-processing

At the data pre-processing stage, p2p, rms, skewness, kurtosis, crest factor and mean features are calculated and used as input to each ML classifier. Each of these features is given below.

2.2.1. Peak to peak

Peak-to-peak is the difference between the highest and the lowest value of the amplitude of a signal. In this study, the p2p value of the vibration signal is calculated and used as input to the classification methods.

2.2.2. Root mean square

The root mean square of a signal is called rms. The rms of a discrete signal or distribution with N samples is given in (6).

$$x_{\text{rms}} = \sqrt{\frac{1}{N} \sum_{i=1}^N |x_i|^2}. \quad (6)$$

2.2.3. Skewness and kurtosis

Skewness is a measure of symmetry in the distribution of a dataset. If the distribution of the dataset looks the same to the right and left of the centre point, it is said to be symmetric. The term “positively skewed” or “right skewed” refers to a distribution concentrated to the left with its tail on the right side. If the distribution is concentrated to the right and with its tail on the left side, it is called a “negatively skewed” or “left skewed” distribution. If the skewness of the distribution is between -0.5 and 0.5 , the results are called to be symmetrical. The data are highly skewed if the skewness is less than -1 or greater than 1 . The skewness of a symmetrical distribution is 0 .

Kurtosis is a measure of outliers present in the distribution of a dataset. It determines whether a dataset has a light or heavy tail compared to normal distribution. Heavy tails or outliers are common in datasets with a high kurtosis value. Low kurtosis datasets tend to have light tails or no outliers. The skewness (s) and kurtosis (k) values of a dataset or a signal (x) can be calculated as given in (7) and (8), respectively.

$$s = \frac{N}{(N-1)(N-2)} \sum_{i=1}^N \frac{(x_i - \mu)^3}{\sigma^3}, \quad (7)$$

$$k = \left(\frac{N(N+1)}{(N-1)(N-2)(N-3)} \sum_{i=1}^N \frac{(x_i - \mu)^4}{\sigma^4} \right) - \frac{3(N-1)^2}{(N-2)(N-3)}, \quad (8)$$

where N is the total number of samples, μ is the mean, and σ is the standard deviation.

2.2.4. Crest factor

Crest factor of a signal is the ratio of the peak value of a signal to its rms value. It is a measurement of the extreme peaks of a signal. The crest factor (cf) of a signal (x) can be calculated by (9).

$$cf = \frac{|x_{\text{peak}}|}{x_{\text{rms}}}. \quad (9)$$

2.2.5. Mean

Mean is the sum of the values of the N sample of a signal divided by the number of samples. It can be calculated as given in (10).

$$\mu = \frac{1}{N} \sum_{i=1}^N x_i. \quad (10)$$

In this study, the rms, p2p, kurtosis, skewness, crest factor, and mean features of the three-axis vibration signals of a three-phase, 3-kW, two-pole IM under 100% loading level are used as input to the k-NN, DT, SVM, and RF classifiers to detect the eccentricity fault. The implementation of the eccentricity fault of IM is given in the next section.

3. Implementation of eccentricity fault

Eccentricity faults occur in IMs due to an imbalanced distance in the air gap between the rotor and stator. Eccentricity faults are classified into static, dynamic, or mixed [37]. The rotor and stator centres are not aligned in static eccentricity.

The dynamic eccentricity fault means that the rotor and the stator centres are not aligned, and the air gap length varies as the rotor rotates. The rotor rotates around both the rotor and stator centres. The mixed eccentricity fault contains static and dynamic eccentricity faults, and the rotor rotates around a centre different from the stator and rotor centres. The types of eccentricity faults are graphically illustrated in Fig. 7.

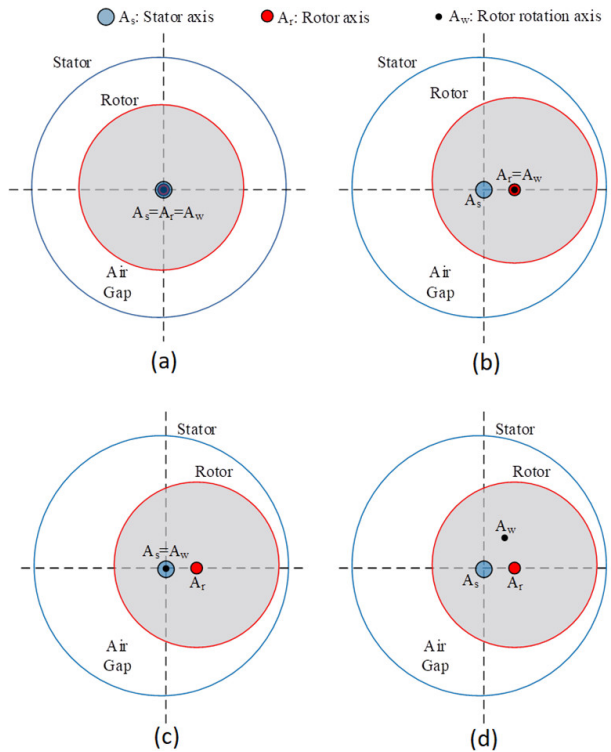


Fig. 7. Types of eccentricity: (a) healthy, (b) static eccentricity, (c) dynamic eccentricity, and (d) mixed eccentricity.

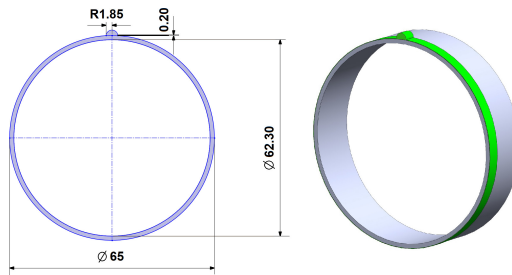


Fig. 8. Dimensions of the designed bushings.

The eccentricity fault analysed in the proposed study has been implemented by widening the housing of the bearings of the IM. The centre of the rotation is shifted 0.2 mm by using bushings produced from a *polylactic acid* (PLA) filament by 3D printing. Figure 8 shows the dimensions of the designed bushings. The details of the implementation of the eccentricity faults are given in [38].

4. Data collection system

A picture of the experimental test bench and the schematics of the data collection system are given in Fig. 9 and Fig. 10, respectively [38, 39]. A two-pole, 3-kW IM was used in the experimental study. A 5-kVA synchronous generator and a variable resistive load were used

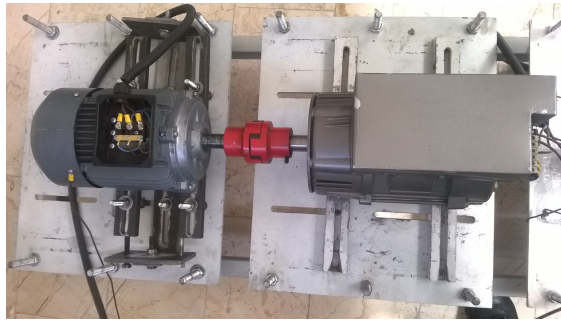


Fig. 9. Experimental test bench.

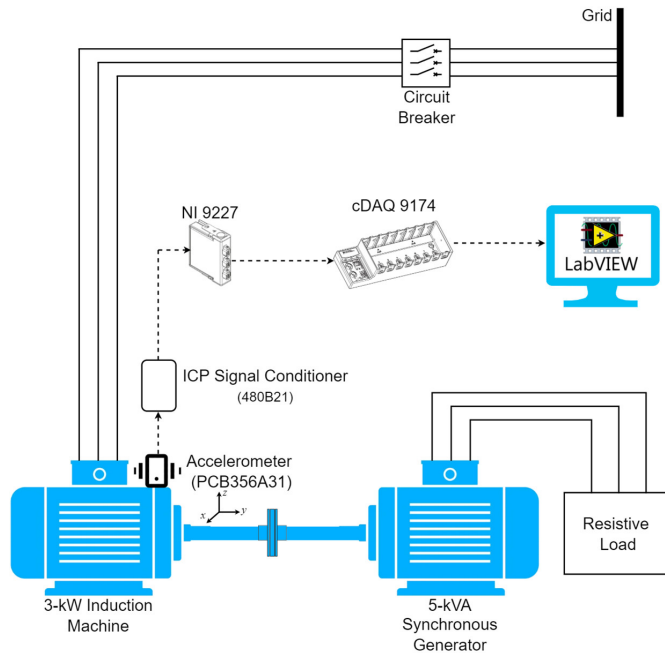


Fig. 10. Schematic of the experimental test bench.

to load the IM. A three-axis accelerometer (PCB356A31), along with an amplifier, were used to measure the vibration signals. The measured vibration signals were recorded by a *National Instrument* (NI) cDAQ 9174 data acquisition system through a NI 9227 module with a sampling frequency of 25 kHz. The data were collected in two test cases. In the first case, the vibration signals were recorded from the motor in a healthy condition. In the second, the vibration signals were recorded from the eccentricity faulty motor. The IM was loaded at 100% and running at 2850 rpm in both cases.

Three-axis (x , y , z) vibration signals were recorded for 41 seconds with a sampling frequency of 25 kHz. The signals were divided into packages of 0.1 seconds (2500 samples). Figure 11 shows the z -axis normalized vibration signal with a duration of 0.1 seconds. The features of each package are calculated, and the results are used to compose a dataset of 410 rows.

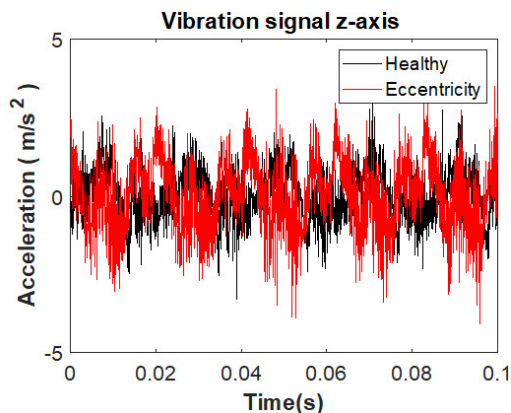


Fig. 11. Z-axis vibration signal.

The p2p, rms, skewness, kurtosis, crest factor, and mean values of the signal were calculated for each row. A dataset with 820 rows (410 rows from healthy motor and 410 rows from eccentricity-faulty motor) representing these features was obtained. Seventy percent (70%) of the dataset was used for training, and 30% of the dataset was used for testing.

5. AutoML

The proposed AutoML model is given in Fig. 12. It is an automated solution to classification problems that reduce the manual efforts of experts in the field of fault detection in IMs. The aim of using AutoML in this study is to fully automate the process of detection of eccentricity fault in IMs by selecting the classifier with the highest accuracy rate and shortest computation time along with the most effective feature(s). In the detection process of faults in IMs it may not be necessary to use many statistical features which require long computational time. Some features may not contribute to the accuracy rate of the detection process of the faults. It may be necessary to detect and/or eliminate the statistical features in the training process that have no significant effect on the accuracy rate of the detection of faults manually in order to reduce the computational time. The proposed AutoML first detects the most effective feature(s). Then it uses these features in the testing process in order to reduce the computational time. Therefore, using the proposed AutoML model reduces the overall computational time of the fault detection process.

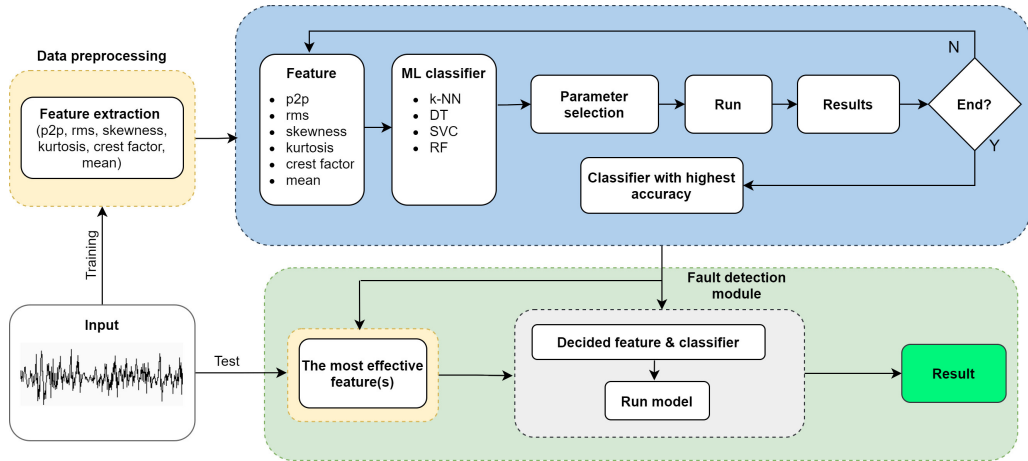


Fig. 12. Proposed AutoML model.

6. Results

An AutoML model was used to diagnose the eccentricity fault of an IM based on three-axis vibration signals (Fig. 12). The AutoML model automatically selects the most effective statistical feature(s) (among p2p, rms, skewness, kurtosis, crest factor, and mean) and the classifier with the highest accuracy and shortest computation time. The fault detection module uses selected statistical feature(s) and classifier as input with the new dataset to detect eccentricity fault.

A confusion matrix was used to assess the performance of each classifier (along with statistical features) run by the AutoML model. The confusion matrices of the classification ML methods of the vibration signals of the z -axis are given in Fig. 13. Label-1 describes the healthy motor, and Label-2 describes the eccentricity-faulty motor. The results show that the rms feature provides the highest accuracy rate (100%) in all four classifiers. It can be seen in Fig. 13 that the k-NN algorithm predicted 97 of 123 data samples of healthy motors correctly, and 26 data samples were predicted incorrectly for the z -axis p2p feature. Out of 123 data samples of the eccentricity faulty motor, 95 were predicted correctly and 28 were predicted incorrectly. Thus, the average accuracy of the k-NN model for the z -axis p2p feature is 78.0488%, as shown in Fig. 13. The accuracy rates of the other classifiers concerning statistical features (p2p, rms, skewness, kurtosis, crest factor and mean) can be seen in Fig. 14.

The proposed AutoML model assesses the performance of the four classifiers based on these results along with the computational time automatically.

The results are given in Table 2 and Fig. 15. It can be seen in Table 2 that 100% accuracy is achieved in all classifiers for the rms feature on the x , y , and z -axis. The variation of the rms level of three-axis vibration signals (healthy and eccentricity faulty) with respect to time is shown in Fig. 16. The p2p and kurtosis features in the x -axis provide 100% accuracy in all classifiers. The DT method with z -axis rms feature provides the highest accuracy rate and the shortest computation time.

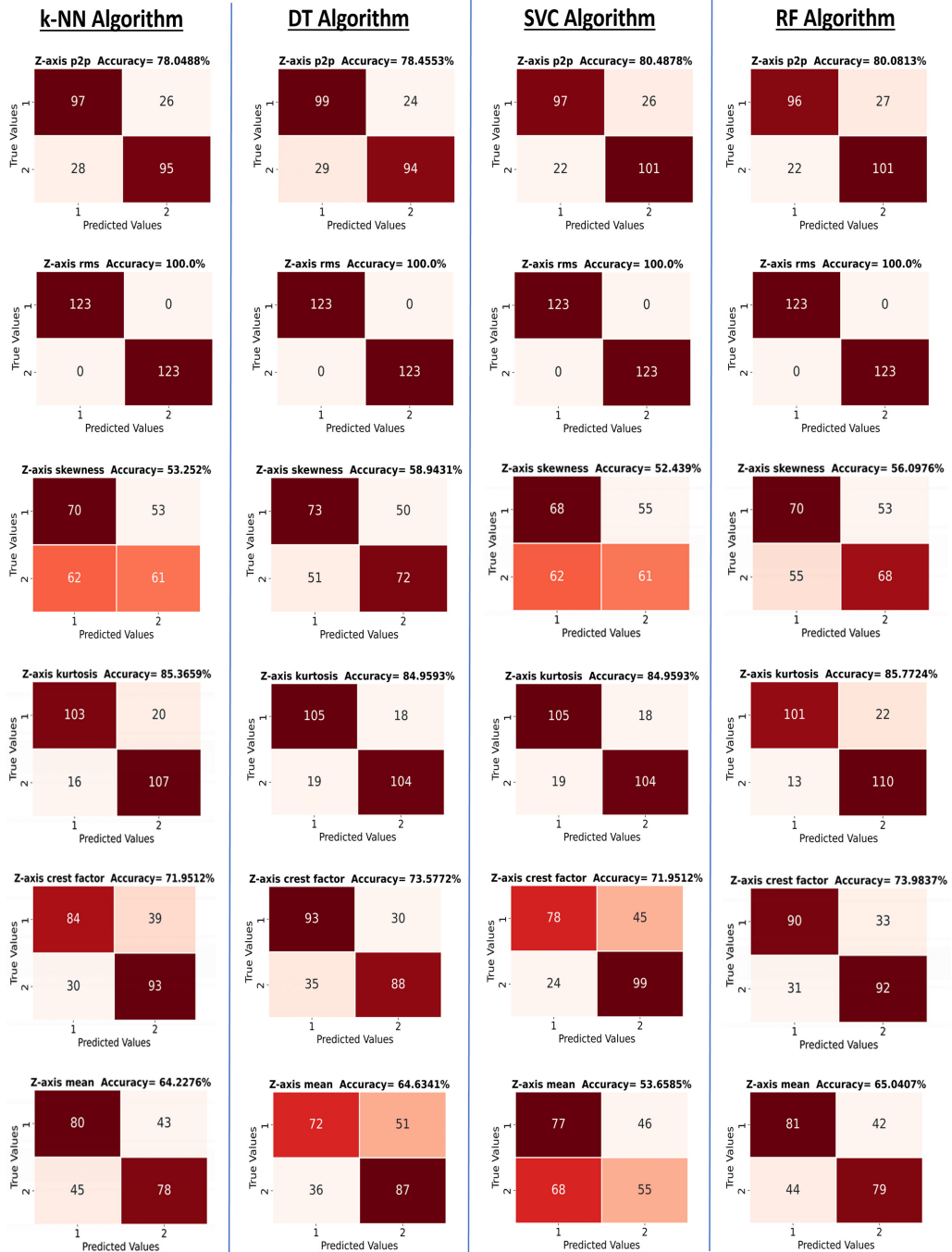


Fig. 13. Z-axis confusion matrix (1: healthy, 2: faulty).

Accuracy rates

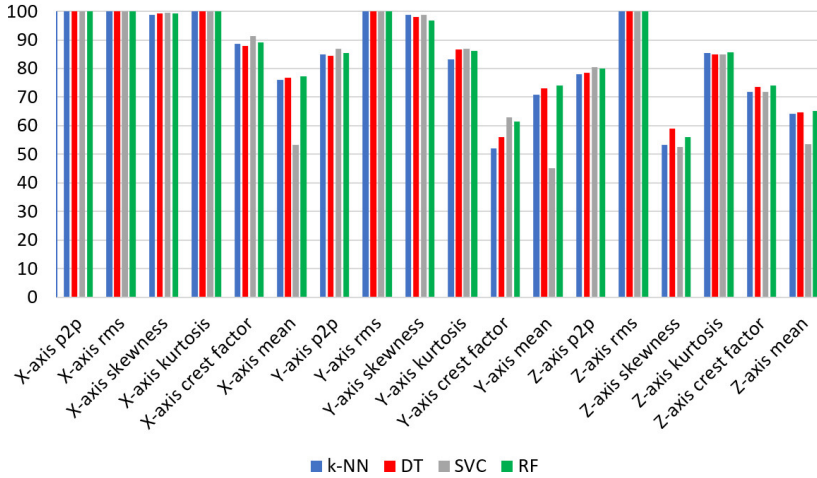


Fig. 14. Accuracy rates of the four classifiers for all features.

Table 2. Accuracy rates and computation times.

Classifiers		k-NN		DT		SVC		RF	
Axis	Features	Acc. %	Computation time (ms)						
x	p2p	100.0	0.27599	100.0	0.41840	100.0	0.81929	100.0	6.45560
	rms	100.0	0.28550	100.0	0.55220	100.0	0.71800	100.0	6.20580
	skewness	98.78	0.48739	99.18	0.76020	99.59	2.51289	99.18	9.66030
	kurtosis	100.0	0.30470	100.0	0.57490	100.0	0.88449	100.0	6.66619
	crest factor	88.62	0.30919	87.80	0.61649	91.46	2.88339	89.02	7.32989
	mean	76.02	0.50439	76.83	0.84809	53.25	6.70240	77.24	7.42250
y	p2p	84.96	0.31549	84.55	0.49739	87.00	3.86299	85.37	7.61540
	rms	100.0	0.39599	100.0	0.50620	100.0	0.89520	100.0	6.63830
	skewness	98.78	0.29029	97.97	0.45840	98.78	1.36980	96.75	6.71940
	kurtosis	83.33	0.30259	86.59	0.55210	87.00	2.55489	86.18	7.06109
	crest factor	52.03	0.28500	56.10	0.71570	63.00	5.70450	61.38	6.96750
	mean	70.73	0.29349	73.17	0.48080	45.12	5.33049	73.98	7.17030
z	p2p	78.05	0.27829	78.46	0.54360	80.49	3.98959	80.08	6.75470
	rms	100.0	0.28330	100.0	0.22620	100.0	0.83749	100.0	6.04900
	skewness	53.25	0.26860	58.94	0.51310	52.44	5.50910	56.10	6.89360
	kurtosis	85.37	0.28739	84.96	0.44789	84.96	2.59359	85.77	6.84169
	crest factor	71.95	0.28320	73.58	0.60120	71.95	4.06170	73.98	7.40819
	mean	64.23	0.27590	64.63	0.55240	53.66	5.34979	65.04	6.88089

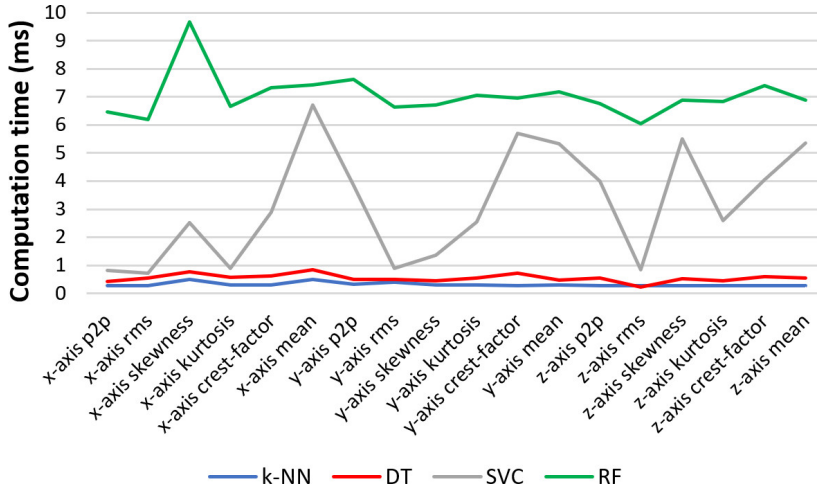


Fig. 15. Computation times of the classifiers with respect to features.

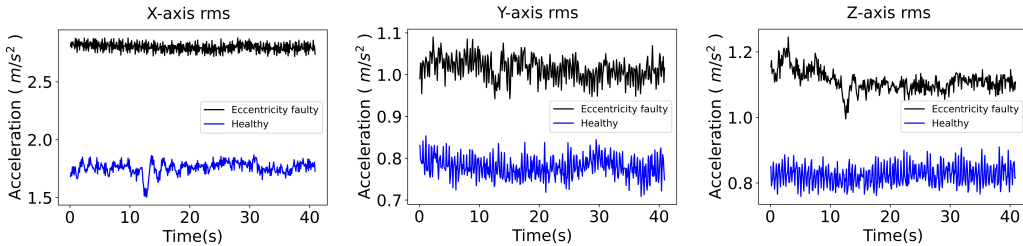


Fig. 16. Rms levels of three-axis vibration signals.

7. Conclusions

Eccentricity faults are among the common mechanical faults in IMs. There are various methods of monitoring and detecting eccentricity faults in IMs. ML methods are among the most effective detection methods. This study proposed an AutoML model that compares the performance of four ML methods, including k-NN, DT, SVC, and RF, in the detection of eccentricity faults in IMs.

The performance of each ML method (as given in Fig. 15) in detecting eccentricity faults was compared with the proposed AutoML model. The classifier with the highest accuracy and the shortest computation time was selected automatically by the proposed AutoML method. The proposed method offers the best ML method with appropriate statistical feature(s) among the four studied algorithms and reduces the need for expert knowledge of ML and eccentricity fault detection.

The results show that the *x*-axis p2p, *x*-axis rms, *x*-axis kurtosis, *y*-axis rms and *z*-axis rms features of the vibration signals provide the highest accuracy rates (100%) in all ML methods. The *y*-axis mean feature provides the lowest accuracy rate in SVC. The SVC classifier gives higher accuracy rates in the *x*-axis crest factor, *y*-axis kurtosis, and *y*-axis crest factor in all ML methods, as shown in Fig. 14. It can also be seen that the accuracy rate of the RF method is higher in the *x*-axis mean, *y*-axis mean, and *z*-axis mean features in all ML methods. The proposed AutoML model offers the DT method and *z*-axis rms feature as input to the fault detection module in this study for the highest accuracy rate and the shortest computation time in the detection of eccentricity fault.

Even though the proposed AutoML model is used for the detection of eccentricity faults in IM by using the four ML methods, it can be used to detect other faults in IMs, including bearing faults, misalignment, and broken rotor bars with other ML methods. In this study, vibration signals are used for the detection of the faults. The proposed model can also be used with other signals, including current, voltage, torque, etc.

Acknowledgements

This work was supported by the Scientific and Technological Research Council of Turkey (TUBITAK) with grant number 116E302.

References

- [1] Gangsar, P., & Tiwari, R. (2020). Signal based condition monitoring techniques for fault detection and diagnosis of induction motors: A state-of-the-art review. *Mechanical Systems and Signal Processing*, 144, 106908. <https://doi.org/10.1016/j.ymssp.2020.106908>
- [2] Bessous, N. (2020). Reliability surveys of fault distributions in rotating electrical machines: – Case study of fault detections in IMs –. *2020 1st International Conference on Communications, Control Systems and Signal Processing (CCSSP)*, 535–543. <https://doi.org/10.1109/CCSSP49278.2020.9151672>
- [3] Bonnett, A., & Yung, C. (2008). Increased efficiency versus increased reliability. *IEEE Industry Applications Magazine*, 14 (1), 29–36. <https://doi.org/10.1109/MIA.2007.909802>
- [4] Liang, X., Ali, M.Z., & Zhang, H. (2020). Induction motors fault diagnosis using finite element method: A review. *IEEE Transactions on Industry Applications*, 56(2), 1205–1217. <https://doi.org/10.1109/TIA.2019.2958908>
- [5] Liu, Z., Zhang, P., He, S., & Huang, J. (2021). A review of modeling and diagnostic techniques for eccentricity fault in electric machines. *Energies*, 14 (14), 4296. <https://doi.org/10.3390/en14144296>
- [6] Alimardani, R., Rahideh, A., & Hedayati Kia, S. (2024). Mixed eccentricity fault detection for induction motors based on time synchronous averaging of vibration signals. *IEEE Transactions on Industrial Electronics*, 71 (3), 3173–3181. <https://doi.org/10.1109/TIE.2023.3266589>
- [7] Wang, B., Lin, C., Inoue, H., & Kanemaru, M. (2022). Topological data analysis for electric motor eccentricity fault detection. *IECON 2022 – 48th Annual Conference of the IEEE Industrial Electronics Society*, 1–6. <https://doi.org/10.1109/IECON49645.2022.9968912>
- [8] Masoumi, Z., Moaveni, B., Mousavi Gazafzudi, S.M., & Faiz, J. (2022). Air-gap eccentricity fault detection, isolation, and estimation for synchronous generators based on eigenvalues analysis. *ISA Transactions*, 131, 489–500. <https://doi.org/10.1016/j.isatra.2022.04.038>
- [9] Amanuel, T., Ghirmay, A., Ghebremeskel, H., Ghebrehiwet, R., & Bahlibi, W. (2021). Design of vibration frequency method with fine-tuned factor for fault detection of three phase induction motor. *Journal of Innovative Image Processing*, 3 (1), 52–65. <https://doi.org/10.36548/jiip.2021.1.005>
- [10] Yu, G. (2020). A concentrated time-frequency analysis tool for bearing fault diagnosis. *IEEE Transactions on Instrumentation and Measurement*, 69(2), 371–381. <https://doi.org/10.1109/TIM.2019.2901514>
- [11] Ahsan, M., & Salah, M.M. (2023). Similarity index of the STFT-based health diagnosis of variable speed rotating machines. *Intelligent Systems with Applications*, 20, 200270. <https://doi.org/10.1016/j.iswa.2023.200270>

- [12] Ehya, Hossein., Nysveen, Arne., & Antonino-Daviu, Jose. A. (2021). Static, dynamic and mixed eccentricity faults detection of synchronous generators based on advanced pattern recognition algorithm. *2021 IEEE 13th International Symposium on Diagnostics for Electrical Machines, Power Electronics and Drives (SDEMPED)*, 173–179. <https://doi.org/10.1109/SDEMPED51010.2021.9605488>
- [13] Liu, Z., Song, Y., Liu, J., Zhang, L., Huang, B., Wu, D., & Liu, J. (2023). Modulation characteristics of multi-physical fields induced by air-gap eccentricity faults for typical rotating machine. *Alexandria Engineering Journal*, 83, 122–133. <https://doi.org/10.1016/j.aej.2023.10.044>
- [14] Neupane, D., & Seok, J. (2020). Bearing fault detection and diagnosis using Case Western Reserve University dataset with deep learning approaches: A review. *IEEE Access*, 8, 93155–93178. <https://doi.org/10.1109/ACCESS.2020.2990528>
- [15] Bousseksou, R., Bessous, N., Zarour, L., Sbaa, S., Pusca, R., Raphael, R., Rezaoui, M.M., Merzouk, I., & Borni, A. (2022). Detailed analysis of rotor eccentricity fault signatures in induction motors using DWT-FFT technique. *2022 19th International Multi-Conference on Systems, Signals & Devices (SSD)*, 74–79. <https://doi.org/10.1109/SSD54932.2022.9955688>
- [16] Boudiaf, R., Abdelkarim, B., & Issam, H. (2024). Bearing fault diagnosis in induction motor using continuous wavelet transform and convolutional neural networks. *International Journal of Power Electronics and Drive Systems (IJPEDS)*, 15 (1), 591. <https://doi.org/10.11591/ijpeds.v15.i1.pp591-602>
- [17] Wang, J., Du, G., Zhu, Z., Shen, C., & He, Q. (2020). Fault diagnosis of rotating machines based on the EMD manifold. *Mechanical Systems and Signal Processing*, 135, 106443. <https://doi.org/10.1016/j.ymssp.2019.106443>
- [18] Kwon, W., Lee, J., Choi, S., & Kim, N. (2024). Empirical mode decomposition and Hilbert–Huang transform-based eccentricity fault detection and classification with demagnetization in 120 kW interior permanent magnet synchronous motors. *Expert Systems with Applications*, 241, 122515. <https://doi.org/10.1016/j.eswa.2023.122515>
- [19] Nishat Toma, R., & Kim, J.-M. (2020). Bearing fault classification of induction motors using discrete wavelet transform and ensemble machine learning algorithms. *Applied Sciences*, 10 (15), 5251. <https://doi.org/10.3390/app10155251>
- [20] Borja, C.A., Tisado, K.J., & Ostia, C. (2022). Fault diagnosis of a brushless DC motor using k-nearest neighbor classification technique with discrete wavelet transform feature extraction. *2022 14th International Conference on Computer and Automation Engineering (ICCAE)*, 122–126. <https://doi.org/10.1109/ICCAE55086.2022.9762425>
- [21] Tang, H., Lu, S., Qian, G., Ding, J., Liu, Y., & Wang, Q. (2021). IoT-based signal enhancement and compression method for efficient motor bearing fault diagnosis. *IEEE Sensors Journal*, 21 (2), 1820–1828. <https://doi.org/10.1109/JSEN.2020.3017768>
- [22] Martin-Diaz, I., Morinigo-Sotelo, D., Duque-Perez, O., & Romero-Troncoso, R.J. (2018). An experimental comparative evaluation of machine learning techniques for motor fault diagnosis under various operating conditions. *IEEE Transactions on Industry Applications*, 54 (3), 2215–2224. <https://doi.org/10.1109/TIA.2018.2801863>
- [23] Kudelina, K., Vaimann, T., Asad, B., Rassõlkin, A., Kallaste, A., & Demidova, G. (2021). Trends and challenges in intelligent condition monitoring of electrical machines using machine learning. *Applied Sciences*, 11 (6), 2761. <https://doi.org/10.3390/app11062761>

- [24] Irgat, E., Unsal, A., & Canseven, H.T. (2021). Detection of eccentricity faults of induction motors based on decision trees. *2021 13th International Conference on Electrical and Electronics Engineering (ELECO)*, 435–439. <https://doi.org/10.23919/ELECO54474.2021.9677809>
- [25] Yatsugi, K., Pandarakone, S.E., Mizuno, Y., & Nakamura, H. (2023). Common Diagnosis Approach to Three-Class Induction Motor Faults Using Stator Current Feature and Support Vector Machine. *IEEE Access*, 11, 24945–24952. <https://doi.org/10.1109/ACCESS.2023.3254914>
- [26] Roy, S.S., Dey, S., & Chatterjee, S. (2020). Autocorrelation aided random forest classifier-based bearing fault detection framework. *IEEE Sensors Journal*, 20 (18), 10792–10800. <https://doi.org/10.1109/JSEN.2020.2995109>
- [27] Stief, A., Ottewill, J.R., Baranowski, J., & Orkisz, M. (2019). A PCA and two-stage Bayesian sensor fusion approach for diagnosing electrical and mechanical faults in induction motors. *IEEE Transactions on Industrial Electronics*, 66 (12), 9510–9520. <https://doi.org/10.1109/TIE.2019.2891453>
- [28] Chen, Y., Rao, M., Feng, K., & Niu, G. (2023). Modified Varying Index Coefficient Autoregression Model for Representation of the Nonstationary Vibration from a Planetary Gearbox. *IEEE Transactions on Instrumentation and Measurement*, 72, 1–12. <https://doi.org/10.1109/TIM.2023.3259048>
- [29] Chen, Y., Rao, M., Feng, K., & Zuo, M.J. (2022). Physics-Informed LSTM hyperparameters selection for gearbox fault detection. *Mechanical Systems and Signal Processing*, 171, 108907. <https://doi.org/10.1016/j.ymssp.2022.108907>
- [30] Mohd Amiruddin, A.A.A., Zabiri, H., Taqvi, S.A.A., & Tufa, L.D. (2020). Neural network applications in fault diagnosis and detection: An overview of implementations in engineering-related systems. *Neural Computing and Applications*, 32 (2), 447–472. <https://doi.org/10.1007/s00521-018-3911-5>
- [31] Zhukovskiy, Y., Buldysko, A., & Revin, I. (2023). Induction motor bearing fault diagnosis based on singular value decomposition of the stator current. *Energies*, 16 (8), 3303. <https://doi.org/10.3390/en16083303>
- [32] Soofi, A.A., & Awan, A. (2017). Classification techniques in machine learning: Applications and issues. *Journal of Basic & Applied Sciences*, 13, 459–465. <https://doi.org/10.6000/1927-5129.2017.13.76>
- [33] da Silva, R.R., & Giesbrecht, M. (2021). Detection of broken rotor bars in induction motors through the k-NN algorithm combined with a deterministic-stochastic subspace method for system identification. *IECON 2021 – 47th Annual Conference of the IEEE Industrial Electronics Society*, 1–6. <https://doi.org/10.1109/IECON48115.2021.9589128>
- [34] Tangirala, S. (2020). Evaluating the impact of Gini index and information gain on classification using decision tree classifier algorithm*. *International Journal of Advanced Computer Science and Applications*, 11 (2). <https://doi.org/10.14569/IJACSA.2020.0110277>
- [35] Al-Qatf, M., Lasheng, Y., Al-Habib, M., & Al-Sabahi, K. (2018). Deep learning approach combining sparse autoencoder with SVM for network intrusion detection. *IEEE Access*, 6, 52843–52856. <https://doi.org/10.1109/ACCESS.2018.2869577>
- [36] Mahami, A., Rahmoune, C., Bettahar, T., & Benazzouz, D. (2021). Induction motor condition monitoring using infrared thermography imaging and ensemble learning techniques. *Advances in Mechanical Engineering*, 13 (11), 168781402110609. <https://doi.org/10.1177/16878140211060956>
- [37] Karampasoglou, D., Bonet-Jara, J., & Gyftakis, K. (2023). Static, dynamic and mixed eccentricity fault detection using MCSA and stray flux monitoring via finite element analysis. *2023 IEEE 14th International Symposium on Diagnostics for Electrical Machines, Power Electronics and Drives (SDEMPED)*, 272–278. <https://doi.org/10.1109/SDEMPED54949.2023.10271409>

- [38] Ünsal, A. (2019). Asenkron motorlar arızalarının tespiti ve entropi analizi ile arıza şiddetinin belirlenmesi (Detection of induction motor faults and determination of fault severity by entropy analysis). TÜBİTAK. <https://search.trdizin.gov.tr/tr/yayin/ara?q=116E302> (2023) (in Turkish). Accessed 26 June 2023
- [39] Kabul, A., & Ünsal, A. (2022). Diagnosis of multiple faults of an induction motor based on Hilbert envelope analysis. *Metrology and Measurement Systems*, 29 (1), 191–205. <https://doi.org/10.24425/mms.2022.138541>



Eyüp Irgat received his B.Sc. from Gazi University in Turkey in 1993 and his M.Sc. degree in Computer and Instructional Technologies from Anadolu University in Turkey in 2002. He is currently pursuing his Ph.D. at the Department of Electrical and Electronics Engineering, Kutahya Dumlupınar University.



Abdurrahman Ünsal received his M.Sc. degree in electrical engineering in 1996 from Oklahoma State University, Stillwater, OK, USA and his Ph.D. degree in 2001 from Oregon State University, Corvallis, OR, USA in electrical engineering. After completing his Ph.D. degree, he joined Kutahya Dumlupınar University as an Assistant Professor at the Department of Electrical and Electronics Engineering. He was promoted to the rank of Associate Professor in 2014. He has been working as a professor in the same department since 2019. His current research interests include power electronics, active filters, fault diagnosis, and electric machines.